American Scientific Research Journal for Engineering, Technology, and Sciences (ASRJETS)
ISSN (Print) 2313-4410, ISSN (Online) 2313-4402

http://asrjetsjournal.org/

Voltage Stability Assessment of Power System with Distributed Generation in Free and Open Source Software

Aung Kyaw Min[a]*, Yan Aung Oo[b]

[a,b]*Department of Electrical Power Engineering, Mandalay Technological University Mandalay, Myanmar*
[a]*Email: aungkyawmin85@gmail.com*
[b]*Email: yanaungoo@gmail.com*

Abstract

This paper presents voltage stability analysis of distributed generation (DG) in mesh distribution network in Power System Analysis Toolbox (PSAT) — free and open source software. Voltage stability analysis of a power system is a necessity, particularly in the planning period of the development or expansion of a power network. The ultimate goal of this paper is to investigate the voltage stability of the 52 buses power system network (Mandalay City) during the expansion of the network. In this paper, a study is being done to expand the power network of the area of Mandalay City. In order to perform the voltage stability analysis, modal analysis as well as PV curves was evaluated based on load flow for selected scenarios. PSAT has been developed to carry out the static voltage stability analysis. And also the dynamic voltage stability analysis has been performed by using time domain simulation with PSAT software.

Keywords: Continuation power flow (CPF); Distributed Generation; modal analysis; Power System Modelling; Voltage Stability.

1. Introduction

Traditionally, electric power is produced at central station power plants and delivered to consumers using transmission and distribution networks. For economic, technical and environmental reasons, there is today a trend toward the use of distributed generation (DG) units in addition to the traditional large generators connected to the transmission system [1]. Thus, it is expected that DGs will have a significant contribution in electrical power systems in the near future.

---

* Corresponding author.

Due to the locally available resources and the small scale, DG units are mostly connected at the distribution level. When the penetration of DG is high, the generated power of DG units not only alters the power flow in the distribution system, but also in the transmission system. As a consequence, the connection of DG to the network may influence the stability of the power system, i.e., angle, frequency, and voltage stability [2], [3]. It might also have an impact on the protection selectivity, and the frequency and voltage control of the system.

Although DG may have some benefits for the system such as improvements in power quality and system efficiency, there are many technical aspects and challenges that are still to be properly understood and addressed. For example, there is a lack of suitable control strategies for networks with significant penetration of DG, while considering the interactions between the transmission and distributions systems. Since most of these studies have to be carried out based on simulations, adequate static and dynamic models for DG units and related interfaces and controls are required. These models should meet certain requirements to allow investigating relevant system stability and control issues, from both local and global system perspectives [4].

The present paper concentrates on studying both static and dynamic DG models for voltage stability studies. These studies do not fully consider the various kinds of DGs. The two types of DG technologies including photovoltaic arrays and PQ synchronous generators are modelled. In these models, both transient and slow dynamics are taken into account. Based on these models, voltage and transient stability studies are carried out. Voltage stability studies are performed based on P-V curves and transient stability studies are performed based on time domain simulation to study contingencies.

Power System Analysis Toolbox (PSAT) [5] is educational open source software for power system analysis studies [6]. The toolbox covers fundamental and necessary routines for power system studies such as power flow, small signal stability analysis, and time-domain simulation. PSAT is a suitable candidate as power system analysis software which is capable of performing core stability analyses.

This paper is organized as follows: section II presents and discusses in detailed the proposed system modelling. In section III, presents system impact study. In section IV, describes the numerical result for a realistic distribution system are presented and discussed. Finally the main conclusions of this work are highlighted in section V.

2. System modelling

The proposed method is tested on the 52 buses power system network (Mandalay City). The test system is shown in figure 1, which contains 52 buses and 48 branches, 11 transformers and 3 generators, 2 of which are hydro generators located in bus 1 and bus 4 whereas the rest is thermal generators located in bus 5. The system has 39 loads, 236.77 MW and 73.114 MVAr, real and reactive power loads respectively. The data used for test system are described in Appendix B.

2.1. DG Allocation

In every case of placement algorithm, optimal DG units are installed in this system. CPF method determines Bus

41 as the most sensitive bus to voltage collapse while modal analysis determines Buses 35, 34, 16 and 18 as critical buses as shown in Table II. Hence, buses 41, 35, 34, 16 and 18 are the DG placement candidates. Figure 8 shows bus 41 as the best candidate for DG placement due to a higher loading parameter. Figure 9 shows an active power production by a settled DG at bus 41 reduces the system losses more than that of a DG at the other buses, providing a higher security margin.

In the second placement round, a CPF analysis introduces bus 34 as the most sensitive bus to voltage collapse while the modal analysis determines buses 35, 16, 18 and 36 as shown in Table IX. By investigating the effects of DG placements, Figure 8 shows that the bigger loadability and more reduction losses are provided when a DG are set at bus 41 and 34. Therefore, these buses are selected as the best location for the second DG. In the third placement DG at bus 18 with two DGs in buses 41 and 34, a CPF shows that the most sensitive bus to voltage collapse is Bus 28, when the modal analysis presents buses 35, 16, 17 and 36 as critical buses (Table IX). Maximum loadability and system losses after DG installation in each candidate bus are shown in Figure 8 and 9, respectively. In the fourth allocation, DG installed at bus 16 with three DG units in buses 41, 34 and 18. Finally, bus 35 is selected as the best place for the fifth DG. The effect of DG placement on the voltage profile is shown in Figure 7.

The proposed placement algorithm is implementable in different DG models as only dispatchable (non-renewable) DG units are connected, only PV DG units are integrated and a mix of dispatchable and PV DG units are connected. Among them implementation of one SPVG model (0.4121 Mw) at bus 35 and four thermal models (25, 12,13 and 5 Mw) at bus 41,34,18 and 16 are the optimal placement respectively shown in figure (8) and (9). A summary of the placement algorithm results along with the evaluation indices for different DG penetration levels are shown in Appendix C.

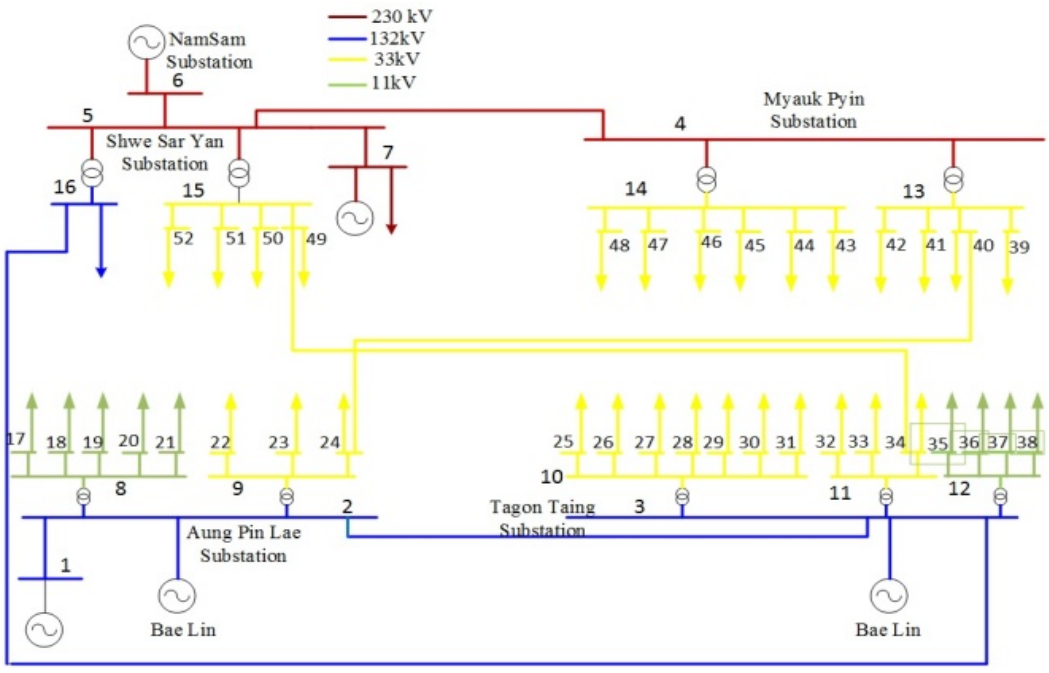

Figure 1: Single line diagram of 52 buses power system network in Mandalay City

2.2. Dynamic Modelling of Hydro and Thermal Generator

Dynamic models of synchronous generators, exciters, turbines, and governors for the proposed power system are implemented in PSAT. All models used are documented in the PSAT Manual. Parameter data for the machines, exciters, and turbine and governors are referred to [8], [9] and provided in Appendix A.

1) Generator Models: Two kinds of synchronous machine models are used in the system: three-rotor windings for the salient pole machines of hydro power plants and four-rotor windings for the round-rotor machines of thermal plants. These two types of generators are described by five and six state variables, respectively. All generators have no mechanical damping and saturation effects are neglected.

2) Automatic Voltage Regulator Models: The same model of AVR, as shown in Figure 2, is used for all generators but with different parameters. The field voltage vf is subject to an anti-windup limiter.

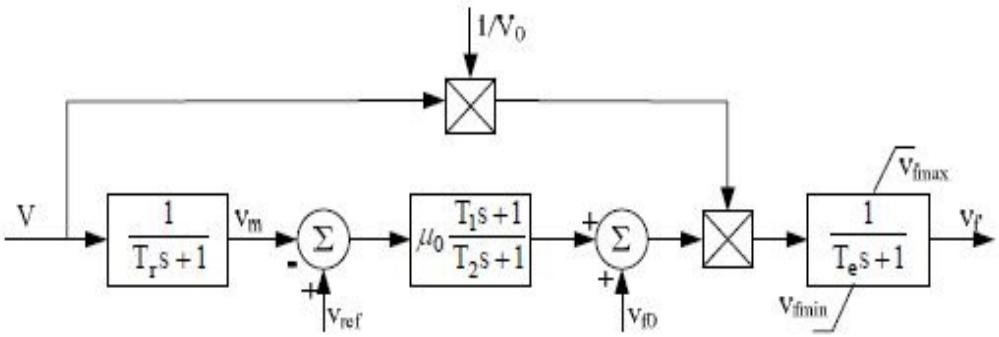

Figure 2: Exciter Model

3) Turbine and Governor Models: In PSAT, there are two models of turbine and governors: namely Model 1 and Model 3. The first one is a thermal generator model while the second is a typical hydro turbine and governor model. As such, the system's hydro generator is represented by Model 3 while that of thermal is represented by Model 1. Block diagrams of these two models are depicted in Figure 3 and Figure 4, respectively.

W. Li and his colleagues recently developed hydro turbine and governor models in PSAT [10]. The block diagram of Model 3 is shown in Fig. 4. Hydro turbine and governor are normally combined together for representation. The block consists of a typical hydro turbine governor and a linearized hydro turbine model where the corresponding elements are depicted in Figure 4.

The linearized turbine is the classical hydro turbine model in power system stability analysis, corresponding to ideal turbine and inelastic penstock with water inertial effect considered. For these models, limits of mechanical torque are checked at the initialization step. It can be also observed those mechanical torques are limits are in p.u. with respect to the mechanical power rating.

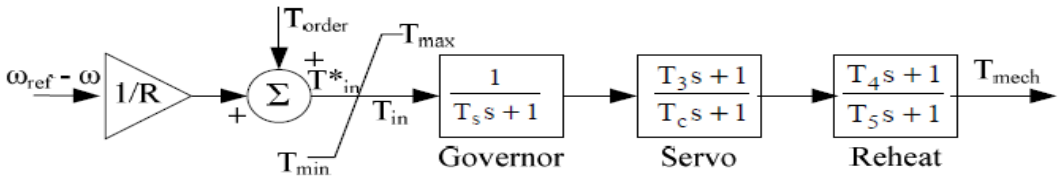

Figure 3: Turbine governor model used of thermal generator: Model 1.

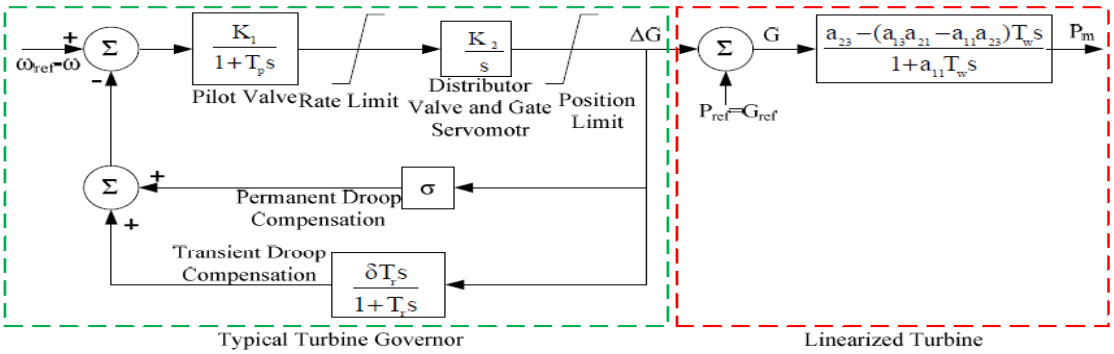

Figure 4: Turbine governor model used for typical hydro generator: Model 3.

2.3. Solar Photovoltaic Generator (SPVG)

This model is based on a current-sourced converter (CSC) as presented in [11]. Two models are used for the photovoltaic source for stability studies based on PQ and PV control models. There are various possibilities for inverter transfer function model, first order transfer functions with steady state gain and closed loop transfer functions are the most appropriate. Since both models yield similar results, the first order transfer function is adopted here.

Figure 5 and Figure 6 present the block diagram of the photovoltaic PQ and PV control models, respectively. In these models, current set point can be obtained based on the desired active and reactive powers and current measurements in the d-q reference frame. All data for the PV and PQ models used here are provided in Appendix A.

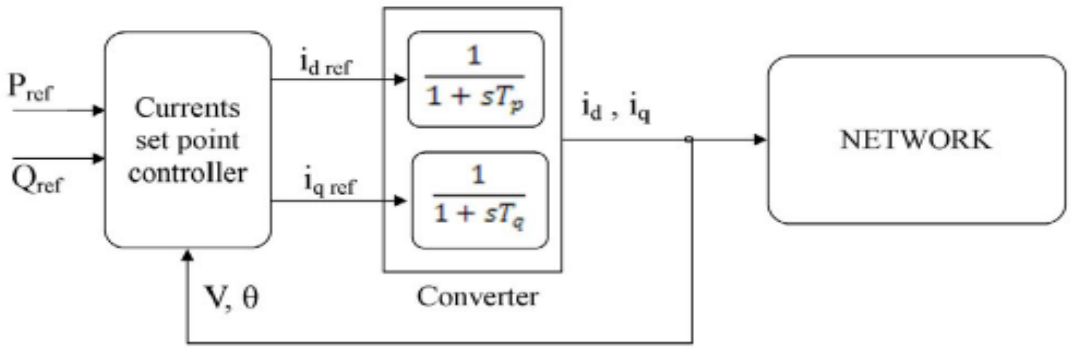

Figure 5: SPVG Model 1 block diagram

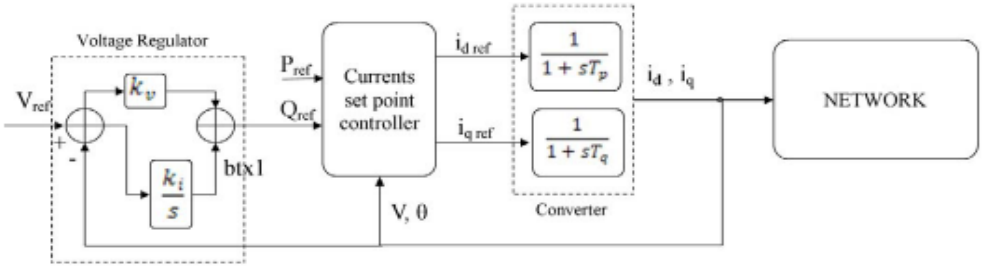

Figure 6: SPVG Model 2 block diagram

3. System impact studies

The main focus of this paper is on stability studies of the system as impacted by DG.

3.1. Voltage stability analysis

Voltage collapse usually occurs in heavily loaded systems that do not have sufficient local reactive power sources and consequently cannot provide secure voltage profile for the system. This reactive power shortage may lead to wide area blackouts and voltage stability problems as has occurred in many countries [14], [15]. The shortage can be relieved by integration of DGs in low voltage (LV) distribution systems to improve voltage stability [17]. These days, most DG technologies, such as synchronous machines, power-electronic interface devices (e.g., photovoltaic cells and micro turbines), and even new induction generators [e.g., doubly fed induction generators (DFIGs)], are capable of providing a fast, dynamic reactive power response. This capability can be used by the system operators to enhance system security and stability. Since a generator location affects the system voltage stability, it is important to identify the most effective buses to install a DG.

3.2. Modal Analysis

The voltage stability problem has a dynamic nature in general, but static analysis techniques are promising tools for predicting the problem characteristics [16]. A modal analysis is as a static approach, it is the best tool for voltage stability analysis. In that modal analysis method can be discovered the instability characteristic effectively. The modal analysis method is used to identify the weakest bus by calculating participation factor and sensitivity factor. Modal analysis ΔV/ΔQ is a powerful technique to predict voltage collapse and determine stability margin in power system. By solving linearized power flow equation we get the ΔP and ΔQ matrix

$$\begin{bmatrix} \Delta P \\ \Delta Q \end{bmatrix} = \begin{bmatrix} J_{P\theta} & J_{PV} \\ J_{Q\theta} & J_{QV} \end{bmatrix} \begin{bmatrix} \Delta\theta \\ \Delta V \end{bmatrix} \tag{1}$$

Considering ΔP = 0, the reduced Jacobian matrix is defined as follow:

$$J_R = \left[J_{QV} - J_{Q\theta} J_{P\theta}^{-1} J_{PV} \right] \tag{2}$$

and

$$\Delta Q = J_R \Delta V \tag{3}$$

$$\Delta V = J_R^{-1} \Delta Q \tag{4}$$

let

$$J_R = \xi \Lambda \eta \tag{5}$$

where

ξ is right eigenvector matrix of ;

η is left eigenvector matrix of ;

Λ is diagonal eigenvalue matrix of .

Then, inverting (5) yields

$$J_R^{-1} = \xi \Lambda^{-1} \eta \tag{6}$$

And substituting (6) and (4) result in

$$\Delta V = \xi \Lambda^{-1} \eta \Delta Q \tag{7}$$

$$\Delta V = \sum_i \frac{\xi_i \eta_i}{\delta_i} \Delta Q \tag{8}$$

where η_i is the i[th] row of the left eigenvector of J_R, and ξ_i is the i[th] column of the right eigenvector. The i[th] mode of the Q-V response is defined by the i[th] eigenvalue δ_i, and the corresponding right and left eigenvectors ξ_i and η_i. Since , (7) may be written as

$$\eta \Delta V = \Lambda^{-1} \eta \Delta Q \tag{9}$$

By defining $v = \Lambda^{-1} q$ as the vector of modal voltage variation and as the vector of modal reactive power variation, one can write uncoupled first-order equations as

$$v = \Lambda^{-1} q \tag{10}$$

Thus, for the i^{th} mode, we have

$$v_i = \frac{1}{\delta_i} q_i \tag{11}$$

If $\delta_i > 0$, the i^{th} modal voltage and the i^{th} modal reactive power variations move in the same direction, indicating voltage stability of the system; whereas $\delta_i < 0$ refers to instability of the system. The magnitude of indicates a relative degree of instability of the i^{th} modal voltage. The smaller the magnitude of a positive δ_i, the closer the i^{th} modal voltage is to being unstable. The system voltage is collapse when $\delta_i = 0$, because any change in the modal reactive power causes an infinite change in the modal voltage.

The relative contribution of the power at bus k in mode i is given by the bus participation factor

$$P_{ki} = \xi_{ki} \eta_{ki} \tag{12}$$

Participation factors determine the most critical areas which lead the system to instability. Usually, the higher the magnitude of the participation factor of a bus in a specific mode, the better the remedial action on that bus in stabilizing the mode.

C. Continuous Power-Flow Methodology

The determination of maximum loading is one of the most important problems in voltage-stability analysis that cannot be calculated directly by modal analysis. Considering a loading scenario, a continuous power flow uses a successive solution to compute the voltage profile up to a collapse point (i.e., where the Jacobian matrix in (1) becomes singular, to determine the voltage security margin (VSM) [17], [18]. The VSM is known as the distance from an operating point to a voltage collapse point [7]. In the successive procedure, the power at the loads increases continuously by a scaling factor as

$$P_L = P_{L0} + \lambda P_D \tag{13}$$

$$Q_L = Q_{Lo} + \lambda Q_D \tag{14}$$

Where P_{L0} and Q_{L0} are load active and reactive powers of the base case whereas P_D and Q_D are the load power direction. The generated power at each generator can be freely scaled by a scaling factor or may be limited by its boundary conditions.

4. Numerical studies

All numerical studies were performed in PSAT [5], which is a MATLAB-based toolbox for power system

studies. It includes power flow, continuation power flow (CPF), optimal power flow, small signal stability analysis and time domain simulation tools. This toolbox also provides a complete graphical interface and a SIMULINK-based one-line network editor.

4.1. System Description

In the system used to test the two DG models (Thermal Generator and SPVG) based on the 52 buses power system network in Mandalay City which is illustrated in Figure 1. Thus, the test system consists of DG units (including prime mover, generator, interface and associated controllers), feeders and loads. The base system load is 236.77 MW and 73.114 MVAr, with the loads being represented using an frequency dependent load (Fl) model, since this model is appropriate for voltage stability studies.

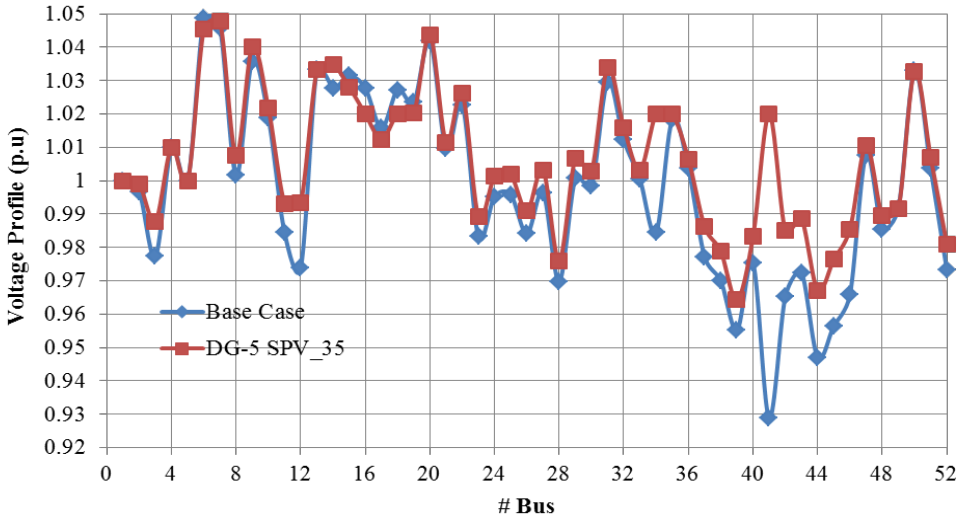

Figure 7: Voltage collapse profile curve in a 52 buses system network

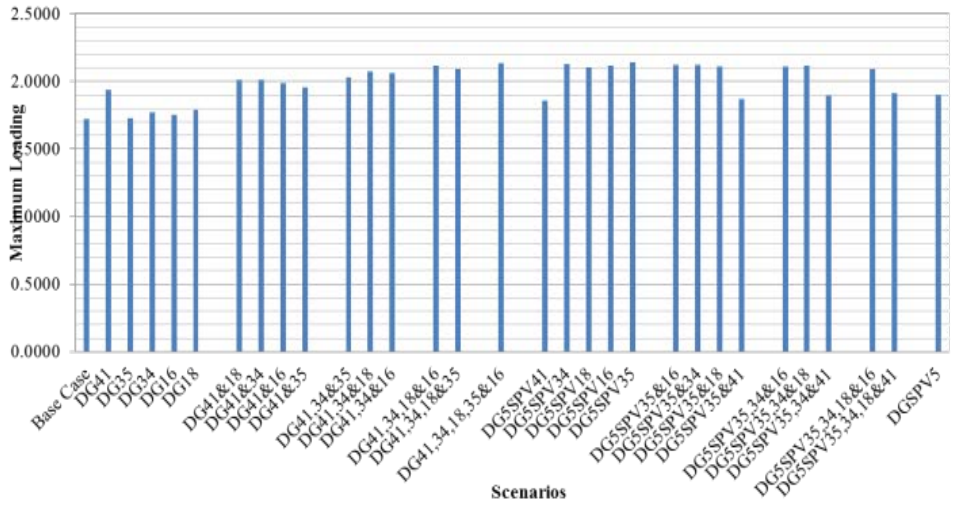

Figure 8: Maximum loading for different placement scenarios

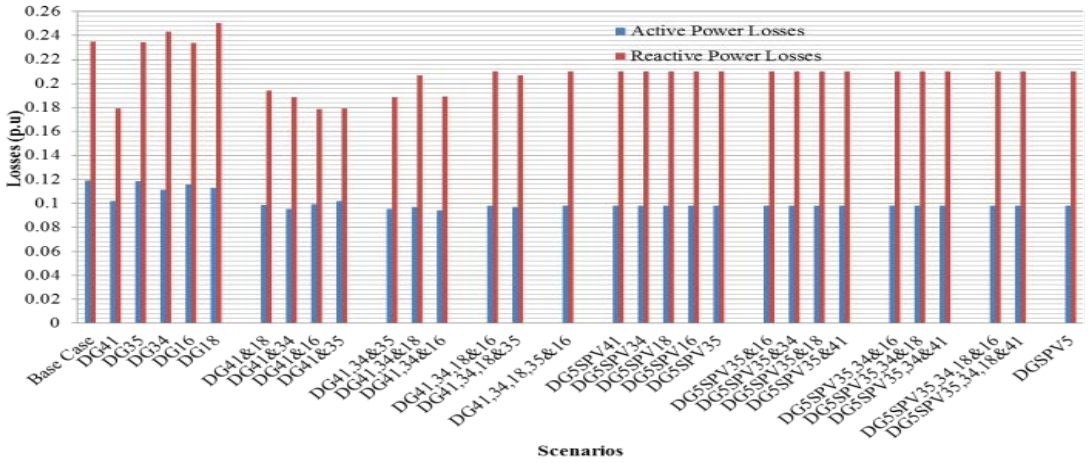

Figure 9: System active and reactive losses for different placement scenarios

4.2. Result and Analysis

1) Voltage Stability

The voltage stability problem has a dynamic nature in general, but static analysis techniques are promising tools for predicting the problem characteristics [16]. Figure 7 shows voltage profile curve in a 52 buses system network.

1.1) CPF and Modal Analysis

The system Jacobian matrix was extracted and reduced to find JR. The magnitude of the eigenvalues as decrease as the system approaches to instability. Then, the eigenvalues of JR were found using the PSAT and the minimum eigenvalues are 0.32819 for DG model (a mix of SPVG and Thermal model) and 0.27737 for Base model. So the base model is more instability than DG model which connected a mix of SPVG and Thermal model.

Table 1: Modal analysis results for the 52-bus system

Eigenvalue	M.P DG Model		M.P Base Model	
δ_1	Bus 35	0.32819	Bus 35	0.27737
δ_2	Bus 35	0.45701	Bus 34	0.41477
δ_3	Bus 36	0.56645	Bus 34	0.46701
δ_4	Bus 17	0.58215	Bus 16	0.47302
δ_5	Bus 31	0.64727	Bus 18	0.52164

M.P –the most participating bus

To know how far the system is from the instability, the minimum eigenvalue of the JR was used to find the participation factor of each bus at this point.

It is not necessary that the lowest voltage bus must be the weakest one. It can be noted that bus 41 has the lowest voltage, but Bus 35 is the weakest bus as participation factor. The participation factor of the bus 35 (least stable mode) is 0.188 for 52 bus system with DG (a mix of SPVG and Thermal model) and in the least stabile mode of the voltage as shown in Figure 10.

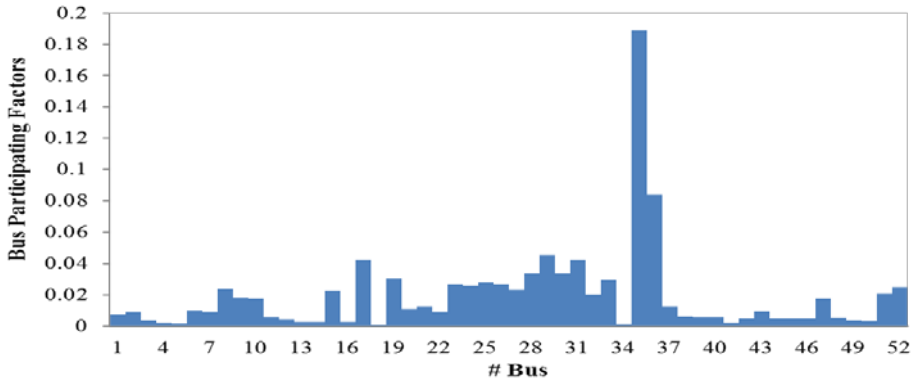

Figure 10: Bus Participation Factors in the least stable mode for 52 bus system with DG (a mix of SPVG and Thermal model

The voltage stability of the system was assessed by examining the system PV curves, which are obtained by increasing the loading level up to the maximum loadability point at which the system experiences voltage collapse [12]. These curves were calculated by using CPF method, which captures the operational limits of all components. Figure 11 and Figure 12 show the PV curves for both base case and DG model (thermal generator and SPVG model) respectively. Improvement of loading parameter by integrating the mix of SPVG and Thermal model is seen in Table II.

Table 2: Objective case

Objective	Base Case	DG Model
P_{losses}	0.119	0.098
Q_{losses}	0.235	0.210
λ	1.7210	2.1419
Voltage collapse Bus By CPF	41	28
Least Voltage Stability Bus By Modal Analysis	35,34,34,16,18	35,35,36,17,31
Bus_ DG Unit		46,44,36,18
PL		23.19%

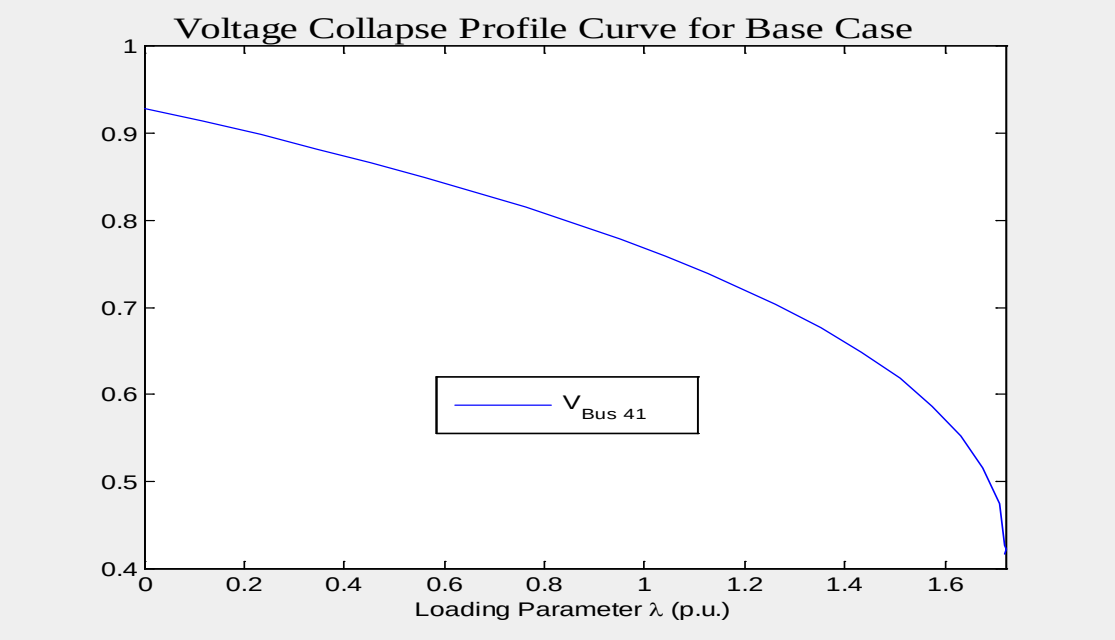

Figure11: Voltage collapse profile for Base model

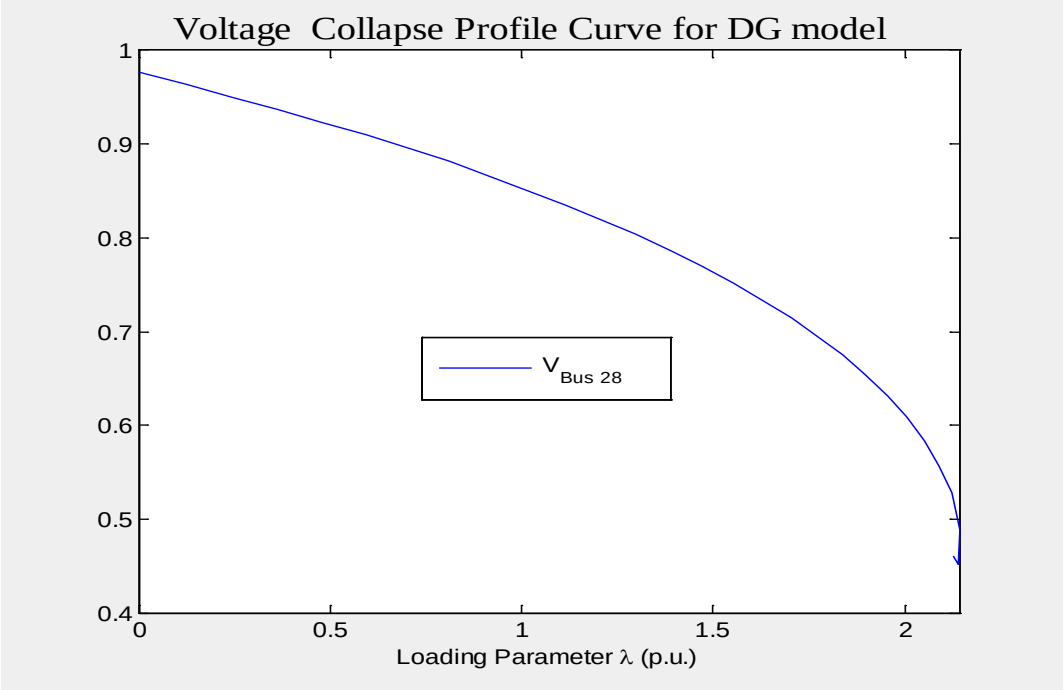

Figure 12: Voltage collapse profile for DG model (a mix of SPVG and Thermal model)

From these curves, the limits of loading at the system are seen clearly. It is maximum loading (1.721 p.u) for base model and 3.1419 p.u for the DG model. Exceeding such limits can cause voltage collapses of the whole system. However, it is clear that the operating point is far enough from the knee points for the current conditions.

2) Time Domain Simulation

In this part, Influence three phase fault on the system is used in order to analyze the dynamic behavior of DG facing with network disturbances. The influence of the three-phase fault on the transient stability of DG is investigated. Five DG ((25, 12, 13, 5 and 0.4121Mw)) are connected at buses 41, 34, 18, 16 and 35, respectively. As such a three-phase fault occurs at bus 22 at T = 1s and removed after 60ms in this study. Figure 13 shows voltages at DG buses for a three-phase fault cleared at T=1.06s (60ms after fault). Figure 14 shows bus voltages due to fault at bus 22.

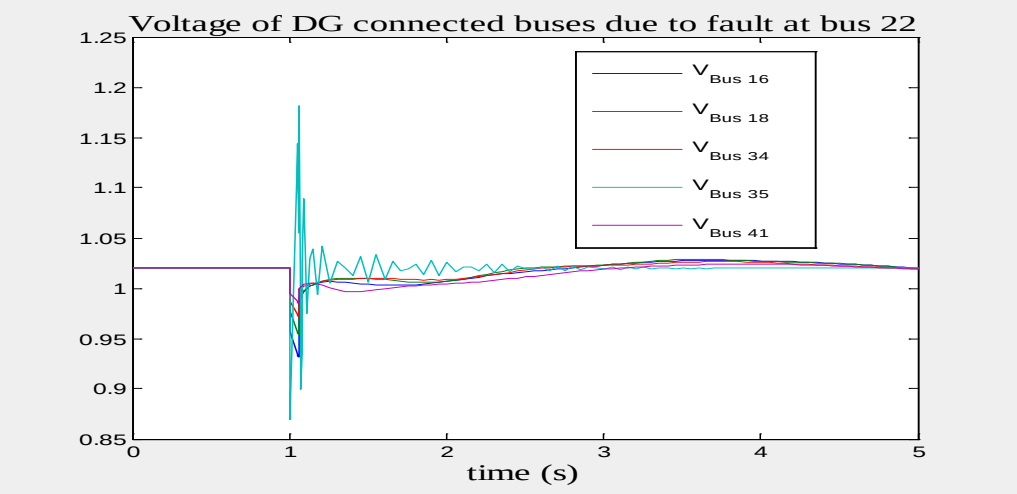

Figure 13: Voltage of DG connected buses due to fault at bus 24

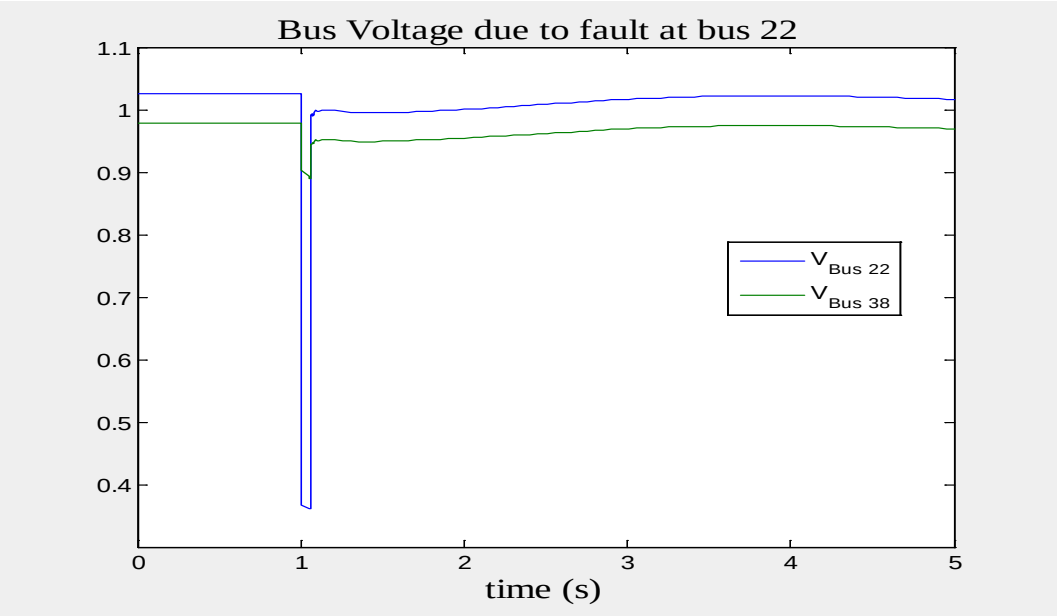

Figure 14: Bus voltages due to fault at bus 24

5. Discussion and conclusion

In this paper, detailed dynamic models of two different DGs are presented. These models contain the dynamic models of the primary governor, generators and their interfaces. Thermal Generator and SPVG model are

modelled and tested by using PSAT.

The DG models were tested and compared using a realistic distribution system to study the static and dynamic behaviour of these models. In this study the voltage stability of the 52 buses power system network (Mandalay City) is presented. The study utilized well-defined techniques to evaluate the voltage stability of a selected the 52 buses power system network (Mandalay City). PV curves are created and the modal analysis technique is used to identify the weakest node in the system. The loadability of the system buses and the weakest bus has been identified. Such results are very important while considering the network expansion and its future operation. The results have been validated via time domain simulations to estimate the system behavior under the disturbance. The voltage stability analysis was evaluated and the time-domain simulation was carried out using PSAT program. It was found that the system would remain stable under the disturbances with short fault clearing time. Further studies are underway to include renewable energy sources. The objective is to consider effect of such distributed resources in the voltage stability of the power system.

Acknowledgments

The author is deeply gratitude to Dr. Myint Thein, rector, Mandalay Technological University, for his guidance and advice. The author would like to thank to Dr. Yan Aung Oo, Professor, Head of Department of Electrical Power Engineering, Mandalay Technological University, for his kind permission, providing encouragement and giving helpful advices and comments. The author is grateful to her paper supervisor, Dr. Lwin Za Kyin, Associated Professor, Department of Electrical Power Engineering, Mandalay Technological University, for her invaluable supervision, helpful suggestion and necessary assistance throughout the preparation of this paper.

References

[1] Jenkins N, Allan R, Crossley P, Kirschen D, Strbac G., Embedded generation, IEE power and energy series: IEE books, 2000.

[2] M.K. Donnely, J. E. Dagel,D.J. Trusnowski, and G.J. Rogers, " Impacts of the distributed utility on transmission system stability," IEEE Trans. Power Syst., vol. 11, no. 2, pp. 741–746, May. 1996.

[3] M. Reza, J. G. Slootweg, P. H. Schavemaker, W. L. Kling, and L.vander Sluis,"Investigating impacts of distributed gene -ration on transmission system stability," in Proc. IEEE Power Tech., Rome, Italy, Jun. 2003.

[4] Ehsan Nasr Azadani and Claudio Canizares, "Modelling and Stability anaylsis of Distributed Generation," IEEE PES General Meeting, July 2012.

[5] F. Milano, "PSAT, Matlab-based Power System Analysis Toolbox," 2002. [Online]. Available: http://www.power. uwaterloo.ca/ fmilano/ downloads.htm.

[6] ——, "An Open Source Power System Analysis Toolbox," IEEE Trans. Power Syst., vol. 20, no. 3, pp. 1199–1206, August 2005.

[7] C. A. Canizares, Ed., "Voltage stability assessment: Concepts, practices and tools," IEEE-PES Power

System Stability Subcommittee Special Publication, SP101PSS, May 2003.

[8] T. Van Cutsem, "Description, Modelling and Simulation Results of a Test System for Voltage Stability Analysis," IEEE Working Group on Test Systems for Voltage stability analysis, Tech. Rep. Version 1, July 2010.

[9] M. C. Stubbe, "Long Term Dynamics Phase II Final Report," Cigre, Tech. Rep. Task Force 38.08.08, March 1995.

[10] W. Li, L. Vanfretti, Y. Chompoobutrgool, "Development and implementation of hydro turbine and governor models in a free and open source software package, Int. J. Simulation Modeling Practice and Theory, vol. 24, pp. 84-102, 2012.

[11] B. Tamimi, C. A. Canizares, and K. Bhattacharya, "Modeling and Performance Analysis of Large Solar Photo-Voltaic Generation on Voltage Stability and Inter-area Oscillations," in Proc. IEEE-PES General Meeting, Detroit,USA, July 2011.

[12] "Voltage stability assessment concepts, practices and tools," IEEE/PES Power System Stability Subcommittee, Aug. 2002.

[13] H. Hedayati, S. A. Nabaviniaki, and A. Akbarimajd, "A method for placement of DG units in distribution networks," IEEE Trans. Power Del., vol. 23, no. 3, pp. 1620–1628, Jul. 2008.

[14] U.S.-Canada Power System Outage Task Force, Final report on the August 14, 2003 blackout in the United States and Canada: Causes and recommendations, Tech. Rep., Apr. 2004.

[15] Federal Energy Reg. Comm., Principles for efficient and reliable reactive power supply and consumption, Feb. 2005.

[16] P. Kundur, Power System Stability and Control. New York: Mc Graw-Hill, 1994.

[17] W. D. Rosehart and C. A. Canizares, "Bifurcation analysis of various power system models," Int. J. Elect. Power Energy Syst., vol. 21, pp. 171–182, Mar. 1999.

[18] V. Ajjarapu and C. Christyl, "The continuation power flow: A tool for steady state voltage stability analysis," IEEE Trans. Power Syst., vol. 7, no. 1, pp. 416–423, Feb. 1992.

Appendix a

Table iii: Parameter of photovoltaic generator

Parameter	*Value*
τ_p*(sec)*	*0.015*
τ_p*(sec)*	*0.015*
K_p	*0.04*
K_i	*20*

Table iv: Generator model parameters

Parameter	Thermal	Hydro
$X_d(pu)$	1.05	1.1
$X'_d(pu)$	0.185	0.25
$X''_d(pu)$	0.13	0.2
$X_q(pu)$	0.98	0.7
$X'_q(pu)$	0.36	0
$X''_q(pu)$	0.2	0.2
$T'_{d0}(sec)$	7	5
$T''_{d0}(sec)$	0.031	0.031
$2H(kWs/kVA)$	13.6	10.296

Table v: Exciter model parameters

Parameter	Thermal	Hydro
$K_a(pu)$	120	50
$T_2\ (sec)$	50	20
$T_1\ (sec)$	5	4
$T_e\ (sec)$	0.1	0.1
$T_r\ (sec)$	0.001	0.001
$v_f^{max}(pu)$	5	4
$v_f^{min}(pu)$	0	0
$v_f^0(pu)$	0	0

Table vi: Turbine governor system model parameters: model 1

Parameter	Value
$R(pu)$	0.04
$T_g\ (sec)$	5
$T_c\ (sec)$	0.2
$T_3\ (sec)$	5
$T_4\ (sec)$	0.01
$T_5\ (sec)$	6
$P_{max}(pu)$	0.95
$P_{max}(pu)$	0

Table vii: Turbine governor system model parameters: model 3

Parameter	Value
T_g *(sec)*	0.2
T_p *(sec)*	0.04
T_r *(sec)*	5
T_w *(sec)*	1
σ*(pu)*	0.04
δ*(pu)*	0.3
a_{11}*(pu)*	0.5
a_{13}*(pu)*	1
a_{21}*(pu)*	1.5
a_{23}*(pu)*	1
G_{max}*(pu)*	1
G_{min}*(pu)*	0

Appendix b

Table viii: load and distribution lines data

Sending Bus	Recceiving Bus	R(pu)	X(pu)	Load at Receiving Bus		Sending Bus	Recceiving Bus	R(pu)	X(pu)	Load at Receiving Bus	
				P(MW)	Q(Mvar)					P(MW)	Q(Mvar)
1	2	0.057	0.088	0	0	12	35	0.678	0.72	2.04	0.63
2	3	0.012	0.019	0	0	12	36	2.082	2.213	3.2	1.3
9	22	0.227	0.287	1.8	0.01	12	37	2.033	2.161	0.044	0.028
9	23	0.379	0.479	8	1.2	12	38	1.598	1.698	1.9	0.2
9	24	0.114	0.144	3.7	1.3	5	4	0.013	0.044	0	0
8	21	1.642	1.381	1.83	1	13	39	0.227	0.287	1.375	0.96
8	20	2.299	1.933	3	0.6	13	40	0.341	0.431	14.2	5.6
8	19	1.971	1.657	1.8	0.95	13	41	0.189	0.24	14.06	5.3
8	18	2.628	2.209	2	1	13	42	0.076	0.096	10.2	3.34
8	17	1.314	1.104	2.1	1	14	43	0.038	0.048	11.75	4.64
2	3	0.012	0.019	0	0	14	44	0.189	0.24	14.76	5.63
3	16	0.021	0.038	0	0	14	45	0.076	0.096	3.27	1.07
10	25	0.124	0.209	12	1.4	14	46	0.227	0.287	15.6	6.23
10	26	0.083	0.139	6	1	14	47	0.17	0.216	14.5	5.67
10	27	0.138	0.232	3.35	0.5	14	48	0.227	0.287	5.22	2.046
10	28	0.186	0.312	7.4	0.7	6	5	0.021	0.057	0	0
10	29	0.044	0.062	6.3	0.65	5	7	0.002	0.008	0	0
10	30	0.394	0.498	6.8	0.68	5	16	0.048	0.086	0	0
10	31	0.467	0.848	0.168	0.01	15	49	0.409	0.685	8.5	5.5
11	32	0.674	0.853	5.375	0.01	15	50	0.383	0.643	5.7	2.21
11	33	1.299	1.092	0.62	0.01	15	51	0.255	0.428	8.248	4.67
11	34	0.124	0.209	6.73	0.24	15	52	0.102	0.171	0.208	0.002

Xappendix c

Table ix: Summary of the placement algorithm results

	ALR	QLR	λ	Candidate Bus By CPF	Candidate Bus By Modal Analysis	Selected Bus	VSM	PL
Base Case	0	0	1.7210	41	35,34,34,16,18		1.7210	
DG41	0.142099	0.236118	1.9366	28	35,34,35,35,18	41	1.9366	10.45
DG35	0.003062	0.001243	1.7291	41	34,34,16,18,36	35	1.7291	0.17
DG34	0.064561	-0.03554	1.7698	41	35,35,16,36,36	34	1.7698	5.23
DG16	0.029436	0.003984	1.7501	41	35,34,35,18,36	16	1.7501	2.01
DG18	0.049152	-0.06607	1.791	41	35,34,35,36,17	18	1.7910	5.32
DG41&18	0.171283	0.173859	2.0097	28	35,16,34,16,36	41&18	2.0097	15.77
DG41&34	0.197862	0.197031	2.0123	28	35,35,16,18,36	41&34	2.0123	15.69
DG41&16	0.167201	0.238557	1.9901	28	35,34,35,18,36	41&16	1.9901	15.77
DG41&35	0.144828	0.237216	1.9543	28	34,34,16,36,36	41&35	1.9543	10.63
DG41,34&35	0.199302	0.197026	2.0329	28	16,16,18,36,17	41,34&35	2.0329	15.62
DG41,34&18	0.187344	0.119883	2.0746	28	35,35,16,36,17	41,34&18	2.0746	20.77
DG41,34&16	0.207098	0.193507	2.0606	28	35,35,18,36,17	41,34&16	2.0606	17.46
DG41,34,18&16	0.177677	0.10533	2.119	28	35,35,36,17,31	41,34,18&16	2.1190	23.02
DG41,34,18&35	0.18742	0.119365	2.0947	28	16,16,36,17,31	41,34,18&35	2.0947	23.02
DG41,34,18,35&16	0.177242	0.104621	2.1376	28	36,36,17,31,19	41,34,18,35&16	2.1376	23.19
DG5SPV41	0.177242	0.104621	1.8602	28	36,17,17,31,19	DG5SPV41	1.8602	23.19
DG5SPV34	0.177242	0.104621	2.1271	28	34,34,17,17,31	DG5SPV34	2.1271	23.19
DG5SPV18	0.177242	0.104621	2.1018	28	18,18,36,17,17	DG5SPV18	2.1018	23.19
DG5SPV16	0.177242	0.104621	2.1146	28	16,16,36,17,31	DG5SPV16	2.1146	23.19
DG5SPV35	0.177242	0.104621	2.1419	28	35,35,36,17,31	DG5SPV35	2.1419	23.19
DG5SPV35&16	0.177242	0.104621	2.1221	28	35,16,16,36,17	DG5SPV35&16	2.1221	23.19
DG5SPV35&34	0.177242	0.104621	2.1253	28	35,35,34,36,17	DG5SPV35&34	2.1253	23.19
DG5SPV35&18	0.177242	0.104621	2.1098	28	35,35,18,17,17	DG5SPV35&18	2.1098	23.19
DG5SPV35&41	0.177242	0.104621	1.8668	28	35,35,36,17,31	DG5SPV35&41	1.8668	23.19
DG5SPV35,34&16	0.177242	0.104621	2.1113	28	35,16,35,34,36	DG5SPV35,34&16	2.1113	23.19
DG5SPV35,34&18	0.177242	0.104621	2.1147	28	35,35,34,18,36	DG5SPV35,34&18	2.1147	23.19
DG5SPV35,34&41	0.177242	0.104621	1.8964	28	35,35,34,36,17	DG5SPV35,34&41	1.8964	23.19
DG5SPV35,34,18&16	0.177242	0.104621	2.0914	28	35,35,16,34,34	DG5SPV35,34,18&16	2.0914	23.19
DG5SPV35,34,18&41	0.177242	0.104621	1.9134	28	35,35,34,18,36	DG5SPV35,34,18&41	1.9134	23.19
DGSPV5	0.177242	0.104621	1.8998	28	35,16,35,34,18	DGSPV5	1.8998	23.19